  Bull. Chem. Soc. Jpn., 59, 127—132 (1986)

Crystal Structure and Physical Properties of (TTM-TTF)$I_{2.47}$

Peiji Wu,† Takehiko Mori,* Toshiaki Enoki, Kenichi Imaeda,
Gunzi Saito,†† and Hiroo Inokuchi
Institute for Molecular Science, Okazaki 444
†† Institute for Solid State Physics, The University of Tokyo, Roppongi, Tokyo 106
(Received June 28, 1985)

The X-ray crystal structure analysis of a novel organic conductor (TTM-TTF)$I_{2.47}$ (TTM-TTF: tetrakis-(methylthio)tetrathiafulvalene) shows that the donors with an almost flat structure are stacked face-to-face to form columns. The iodine lattice composed of I_3^- columns is incommensurate with the donor lattice. The measurements of resistivity, thermoelectric power, and ESR show a metal-insulator transition around 100 K. This transition is attributed to the Peierls type phase transition. The quasi-one-dimensional electronic structure is supported by the arrangement of the donor molecules in the crystal and the calculated anisotropy of transfer integrals.

It has been demonstrated that in organic conductors an enhancement in the dimensionality is required to stabilize the metallic states and to design organic superconductors. Among the organic conductors including BEDT-TTF (bis(ethylenedithio)tetrathiafulvalene), two-dimensional conductors which are metallic down to liquid helium temperature and even superconductors have been discovered.[1-3] The investigations of the crystal structures and electronic structures have indicated that the side-by-side intermolecular interaction of these BEDT-TTF compounds is comparable to a face-to-face interaction.[4-6] This characteristic property is considered to come from the four outer sulfur atoms attached to the tetrathiafulvalene(TTF) skeleton. For the purpose of developing organic donors directed toward organic superconductors, it is important to investigate the influence of the outer alkyl groups in other alkylthio-substituted TTF's on the dimensionality of the electronic systems.

As a part of the investigation of uncapped tetrakis(alkylthio)-substituted TTF (TTC_n-TTF) (Scheme), where "uncapped" means that each outer ethylene group of BEDT-TTF is replaced by two separated alkyl groups, we have prepared a variety of charge-transfer complexes including tetrakis(methylthio)tetrathiafulvalene (TTC_1-TTF=TTM-TTF).[7,8] Among them the iodine complex (TTM-TTF)I_x showed the highest conductivity. In the present report, we deal with the crystal structure, electric conductivity, thermoelectric power, ESR spectra, and electronic structure of this iodine complex.

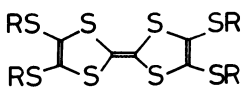

TTC_n-TTF R=C_nH_{2n+1}
TTM-TTF R=CH_3

Scheme.

† On leave from the Institute of Chemistry, Academia Sinica, Beijing, China.

Experimental

The iodine complex was prepared by the following three methods; (1) electrocrystallization of the donor with tetrabutylammonium triiodide as an electrolyte in a mixed solvent of benzene and methanol, (2) direct mixing of the donor and the electrolyte in dichloromethane and methanol, and (3) direct reaction of the donor with iodine molecules in dichloromethane and methanol.

X-Ray photographs with the use of Cu $K\alpha$ radiation confirmed that all these methods gave the same complex. The results of elemental analysis showed the iodine/donor ratio x to be close to 5/2 or 12/5. The exact estimation by means of an X-ray investigation indicated x=2.47. Anal. Calcd for $C_{10}H_{12}S_8I_{2.47}$: C, 17.11; H, 1.72; S, 36.53; I, 44.64. Found: C, 16.91; H, 1.73; S, 36.95; I, 44.67.

Oscillation photographs along the crystal needle axis displayed ununiformly spaced layer lines (Fig. 1), which indicated the presence of a superlattice structure characteristic of iodine complexes.[9] This superlattice structure was considered to be composed of donor and iodine subcells. Among these layer lines the scatterings from the iodine subcell were neglected in the course of the structure analysis.

The intensity data of the donor subcell were collected at room temperature with a Rigaku automated four circle diffractometer using monochromatized Mo $K\alpha$ radiation by the ω-2θ scan technique. Since the intense scatterings from the iodine subcell were neglected and the iodine subcell was approximately commensurate with the donor subcell, the accuracy of the intensity data was limited. Only 664 independent reflections of 2112 accessible reflections ($2\theta \leq 50°$) were recorded with sufficient accuracy ($|F_o| \geq 3\sigma(|F_o|)$). Cell parameters were determined from least squares applied to 25 reflections with $25° < 2\theta < 30°$.

In the course of the structure determination, first the b-axis projection, which corresponds to the projection along the crystal needle axis, was deduced from the Patterson systhesis using the $h0l$ reflections. Since the $h0l$ reflections of the donor subcell was common to that of the iodine subcell, the position of the iodine column in the b axis projection was also determined. Then the three-dimensional structure was derived from this projection. In

Table 1. Atomic Parameters

Atom	$X(\times 10^4)$	$Y(\times 10^3)$	$Z(\times 10^4)$
I	287(3)	—	3589(4)
S(1)	1747(3)	437(3)	161(4)
S(2)	3045(3)	453(3)	971(3)
S(3)	1485(3)	763(3)	1215(4)
S(4)	2906(4)	799(3)	2094(4)
C(1)	2461(10)	293(10)	250(13)
C(2)	1996(11)	635(10)	948(14)
C(3)	2599(11)	625(9)	1332(13)
C(4)	781(16)	635(10)	523(21)
C(5)	3681(12)	684(8)	2363(15)

the three-dimensional structure analysis the iodine atoms were considered to be distributed randomly along the b direction. The three-dimensional structure was refined by the block diagonal least squares method. Anisotropic thermal parameters were adopted for non H atoms. Hydrogen atoms were not included in the refinement. Final refinement gave R=0.099 and R_w=0.126, where $w=1/[\sigma^2(F_o)+0.000225F_o^2]$. The positional parameters are listed in Table 1. The F_o—F_c table and the anisotropic temperature parameters are deposited as Document No. 8604 at the Office of this Bulletin.

The dc resistivity of the single crystal was measured by the four-probe method using gold paint. The anisotropy of the resistivity was measured by the combined use of the Montgomery method and the two-probe method. The thermoelectric power along the b axis was measured by attaching a single crystal with gold paint or carbon paint to two boron nitride heat sinks.[10] ESR data were obtained with an X-band spectrometer Varian E112 equipped with an Oxford Instruments ESR 9 continuous flow helium cryostat.

Results

Among the ununiformly spaced layer lines of the oscillation photograph along the crystal needle axis, the layer line with a spacing of 3.978 Å was attributed to the donor subcell, because the observed high conductivity suggests that the donor molecules form a columnar structure along the crystal needle axis. Weissenberg photographs and the investigation using a four-circle diffractometer determined the crystal data of the donor subcell to be: monoclinic, $C2/c$, a=24.78(1), b=3.978(2), c=22.65(1) Å, β=115.50(5)°, V=2015(2) Å^3, and Z=4. The b axis corresponds to the crystal needle axis.

Iodine species reported to exist in solids include I_2, I^-, I_3^-, I_5^-.[9] In addition to the scatterings from the donor subcell, the oscillation photograph along the b axis displayed layer lines at 0.233, 0.412, 0.823, 1.234, and 1.647 reciprocal lattice units of the donor subcell, b/d (Fig. 1). All these layer lines were composed of well-defined spots even at room temperature, and no diffuse layer was observed. This observation indicates the three-dimensional order of the iodine atoms.

The layer lines at 0.233 and 1.647 are weaker than the donor layer lines and the layer lines at 0.412 and 0.823 are weaker still. The layer line at 1.234 is comparable to that of the donor subcell and is attributed to the average spacing of the iodine atoms along the b axis. Since the resulting atom spacing 3.224 Å is shorter than twice of the I^- ionic radius, 4.3 Å, the presence of an I^- column is excluded. This is also consistent with the supposition that if the iodine existed as I^-, the charge on the donor should be unrealistically large.

The layer lines at 0.412, 0.823, 1.234, and 1.647 form a series with a lattice constant b'=9.670(6) Å. This lattice constant is three times as large as the above-mensioned iodine average spacing. It is documented that I_3^-, which is the most common iodine species, has a repeat period of 9.4—9.7 Å in the iodine column.[9] Therefore, this subcell spacing indicates the presence of the I_3^- column. The existence of the I_5^- column, which displays a repeat period of about 15.5 Å,[9] is excluded.

The layer line at 0.233 is not due to the two-fold structure of this iodine subcell which should appear at 3.978 Å/2×9.670 Å=0.206. This layer line is attributed to the convolution of the intense iodine layer line and the donor layer line, b/d=1.234—1.0= 0.234.

The ratio of b to b′ determines the iodine content to be $x=6b/b'$=2.468(3). The scatter of x among the samples prepared by different methods is too small to be detectable by X-ray investigations. The stoichiometry associated with x=2.47 is between TTM-TTF_5I_{12} (x=2.4) and TTM-TTF_2I_5 (x=2.5); the iodine subcell is incommensurate with the donor subcell.

Since no additional scattering is found in the k=0 Weissenberg photograph, the iodine subcell corresponds to the donor subcell in the a*c* plane. The crystal data of the iodine subcell were determined by the combined use of Weissenberg photographs and a four circle diffractometer: triclinic, a'=24.97, b'=9.670, c'=48.95 Å, α'=111.55, β'=112.38, γ'=94.60°, and V=9827 Å^3. This subcell is related to the donor subcell by the equations: **a*′=a***, **b′//b**, **2c*′=c***.

The 5th layer line of the iodine subcell at 2.06 was not clearly distinguishable from the second layer of the donor subcell. Moreover the iodine subcell gave poorer quality scatterings than did the donor subcell. Therefore analysis of the intensity data was not attempted for the iodine subcell.

The crystal structure is shown in Figs. 2 and 3. The donor molecule TTM-TTF is almost flat similarly to other TTM-TTF complexes such as (TTM-TTF)(HCBD) and (TTM-TTF)AsF_6,[7,8] although its neutral structure is strongly deformed to be nonplanar.[8] The donor molecules are stacked

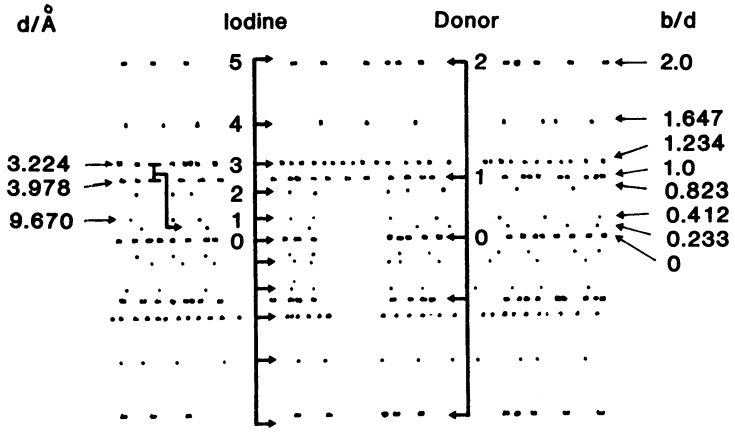

Fig. 1. Schematic representation of the oscillation photograph along the b axis. On the right side is shown b/d: the inverse of d (Å), multiplied by $b=3.978$ Å.

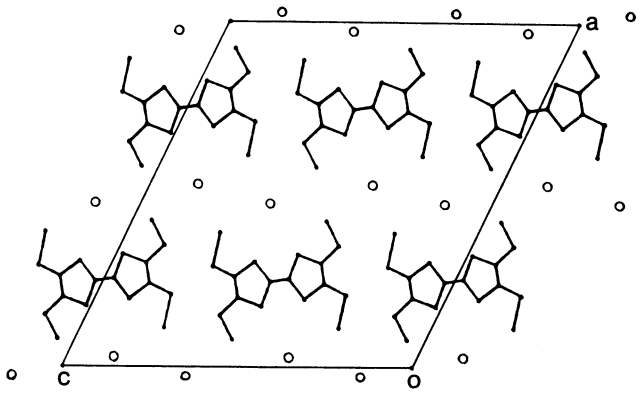

Fig. 2. Crystal structure: projection along the b axis. The white circles designate ioldine columns.

face-to-face to form a column along the b axis. The interplanar spacing is 3.58 Å and there is no shorter sulfur-to-sulfur contact than the van der Waals distance (3.7 Å) (Fig. 3). The mode of intermolecular overlap is, however, favorable to the orbital overlap (Fig. 4);[5] the adjacent molecules are displaced from each other by 1.37 Å along the long molecular axis.

There are comparatively short intercolumnar sulfur-to-sulfur contacts between the outer sulfur atoms (Fig. 3). The donor molecules form conducting sheets parallel to the bc plane in association with the short sulfur-to-sulfur contacts, and these sheets are separated from each other by the anions. The long axis of the molecule is almost parallel to this sheet.

This exhibits a striking contrast to the BEDT-TTF compounds. In all BEDT-TTF complexes whose crystal structures have been known so far, the molecular long axis is almost perpendicular to the sheet, and the intermolecular contacts at the molecular long sides are as important as the face-to-face interaction for the electron transfer.

As for TTM-TTF the terminal methyl groups extending to the direction perpendicular to the molecular long axis (see Fig. 2) block the contacts at the molecular long sides. In addition, the presence of the anions are also disadvantageous for the intermolecular interactions perpendicular to the molecular long axis in the ac plane. Since the outer sulfur atoms are instead exposed to the adjacent donors at the molecular short sides, the sheet of the donors extends through the contacts at the molecular short sides.

The b axis resistivity is shown in Fig. 5. The resistivity at room temperature is in the range of 7—10×10^{-3} Ωcm. The resistivity slightly decreases as the temperature is lowered down to 155 K, where it exhibits a broad minimum. Below 100 K the resistivity steeply increases in an activated manner with $E_a=0.028$ eV. The anisotropy of the resistivity is estimated to be $\rho_b:\rho_c:\rho_a=1:50:4000$.

The thermoelectric power is negative (−9 μV/K) at room temperature and decreases slightly to 155 K (−10 μV/K) (Fig. 6). Around this temperature the thermoelectric power has a broad minimum and increases below this temperature.

The magnetic susceptibility associated with the ESR intensity is almost constant from room temperature to 155 K (Fig. 7). In the temperature region between 155 and 100 K, the susceptibility decreases, but the temperature dependence is too gradual to be fitted to an activation-type formula. Below 100 K the susceptibility behaves in an activated manner with $E_a=0.022$ eV. This value agrees with the activation energy of the resistivity in this temperature region. Judging from the behavior of both the resistivity and the susceptibility, a metal-insulator transition is considered to take place at $T_c=100$ K.

The ESR linewidth is 56 G at room temperature and with a decrease in temperature decreases linearly

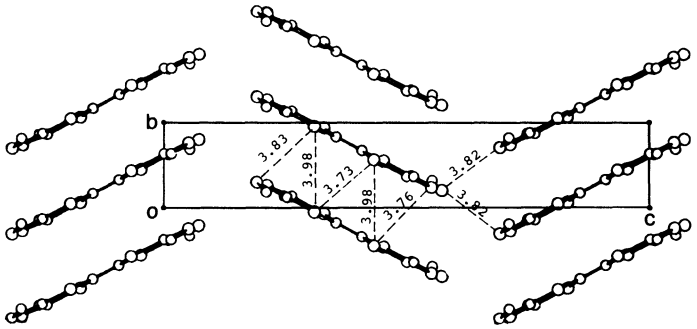

Fig. 3. Crystal structure: projection along the a axis and short intermolecular sulfur-to-sulrfur distances.

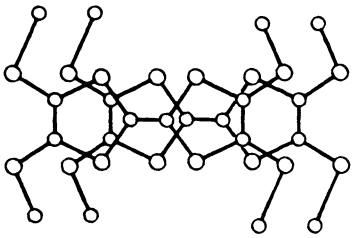

Fig. 4. Mode of the intracolumnar overlap of the TTM-TTF molecules.

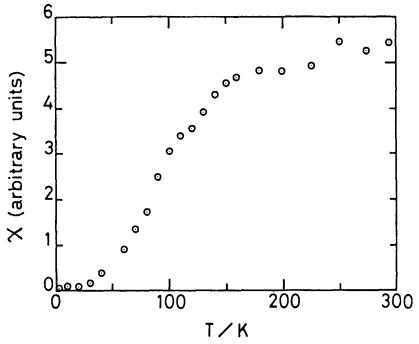

Fig. 7. Temperature dependence of the relative spin susceptibility χ.

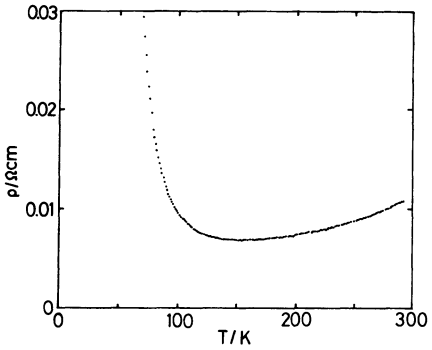

Fig. 5. Temperature dependence of the electrical resistivity ρ along the b axis.

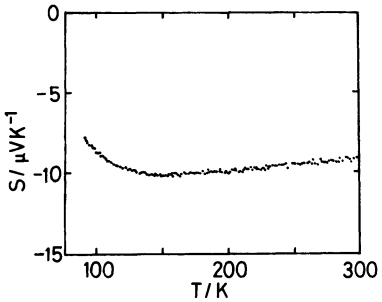

Fig. 6. Temperature dependence of the thermoelectric power S along the b axis.

like that of other halides and pseudohalides of TTF derivatives.[11] This large linewidth suggests the presence of conducting sheets where the spin relaxation is allowed through interchain hoppings. The g-value (H//a*) is almost constant (2.003) through all the measured temperature region, and is close to the free electron value.

Discussion

From the stoichiometry (TTM-TTF)$I_{2.47}$ and the presence of the I_3^- species established by the X-ray investigation, the charge on a donor molecule is estimated to be n=0.823. This value is consistent with that in the estimation from the intramolecular bond lengths of the donor.[4] In general TTM-TTF tends to be slightly more positively charged in charge-transfer complexes in comparison with BEDT-TTF.

In order to estimate the anisotropy of the electron transfer, intermolecular overlap integrals of the highest occupied molecular orbital (HOMO) have been calculated on the basis of molecular orbital calculations.[5,6] The intermolecular overlap in the column is -14.7×10^{-3} and the intercolumnar overlap along the c axis is 0.88×10^{-3}. If transfer integrals t are assumed to be proportional to the intermolecular

overlaps, the anisotropy of the transfer integrals are obtained, $t_c/t_b=0.06$.

In a quasi-one-dimensional band, the ratio of the conductivity is roughly proportional to the square of the transfer integrals,[12] $(\sigma_c/\sigma_b)\simeq(ct_c/2bt_b)^2$. Thus σ_c/σ_b is evaluated to be 0.03, in agreement with the observed anisotropy 0.02.

The dimensionality of this TTM-TTF complex is lower than that of ordinary BEDT-TTF complexes. Then it is convincing that the metal-insulator transition at $T_c=100$ K observed in the resistivity and the magnetic susceptibility is attributed to the Peierls type phase transition in the quasi-one-dimensional donor chain.

A surprising observation concerning this complex is the negative thermoelectric power at high temperatures. Halide and pseudohalide systems of the TTF family ordinarily show positive thermoelectric power, because of the hole carriers existing on the donors. In a simple tight-bindihg band the thermoelectric power changes its sign to the band center, which corresponds to the degree of charge transfer $n=1.0$. In (TTM-TTF)$I_{2.47}$, the relatively large degree of charge transfer $n=0.823$ causes the Fermi energy E_F near to the band center. Thus it is possible that the deviation of the energy band from the simple tight-binding band brings about a positive curvature at E_F in the band, leading to the negative thermoelectric power.

The negative thermoelectric power is, however, attributable to the presence of a pseudogap generated by the fluctuation in the iodine lattice. Since the iodine lattice has three-dimensional order even at room temperature, a pseudogap at E_F is induced by the periodical potential of the iodine atoms. The electronic structure at high temperatures is rather semimetallic or narrow-gap semiconductor-like than one-dimensional metallic. Such an electronic structure makes the thermoelectric power either positive or negative, depending on the difference of the carrier mobilities above and below the pseudogap.

The small increase in the resistivity and the gradual decrease in the spin susceptibility blow 155 K suggest the precursor effect of the Peierls transition. Since the iodine lattice is approximately commensurate with the donor lattice, the possibility remains that a lock-in transition may take place. The X-ray investigation which determined the average periodicity of the iodine lattice does not exclude the existence of minor iodine species other than I_3^-. Therefore, the degree of charge transfer may be changed a little from $n=0.823$, depending on temperature. Then the phase transition is possibly cooperated with the change of order in the iodine lattice and/or the degree of charge transfer. In order to confirm this speculation temperature-dependent investigation of charge transfer is desirable by means of X-ray analysis or Raman spectroscopy.

It has been suggested that the spread of the donor HOMO is related to the dimensionality of the complex.[13] As the ratio of the atomic populations of the HOMO between the outer sulfur atoms and the inner sulfur atoms P_2/P_1 increses, the dimensionality is enhanced through the increase in the transverse intermolecular overlap. The ratio P_2/P_1 is calculated to be 0.452 for TTM-TTF. This value is even larger than the 0.148 for BEDT-TTF and the 0.315 for BMDT-TTF which form conductors with two-dimensionality.[14] In TTM-TTF, however, the transverse interaction at the molecular long sides is inhibited by the methyl groups; the transverse interaction works only through the outer sulfur atoms at the molecular short sides. Thus the magnitude of the transverse interaction is small. This is the reason for the less than two-dimensional electronic structure of this TTM-TTF complex, in spite of a large P_2/P_1.

In conclusion (TTM-TTF)$I_{2.47}$ is recognized as a quasi-one-dimensional conductor with an incommensurate iodine superlattice. Since the iodine atoms have three-dimensional order, the electronic structure at room temperature is considered to be semimetallic or narrow-gap semiconductor-like. Thus the resistivity shows a slightly metallic temperature dependence, the spin susceptibility is almost constant, and the thermoelectric power shows a negative value with small temperature dependence. Around $T_c=100$ K a metal-insulator transition takes place, which is attributed to the Peierls type instability. The arrangement of the donor molecules in the crystal and the calculated anisotropy of the transfer integrals support a comparatively one-dimensional electronic structure of this complex.

The authors are grateful to Prof. H. Kobayashi and Dr. A. Kobayashi for helpful advice on the structure analysis.

References

1) G. Saito, T. Enoki, K. Toriumi, and H. Inokuchi, *Solid State Commun.*, **42**, 557 (1982).

2) S. S. P. Parkin, E. M. Engler, R. R. Schumaker, R. Lagier, V. Y. Lee, J. C. Scott, and R. L. Greene, *Phys. Rev. Lett.*, **50**, 270 (1983).

3) E. B. Yagubskii, I. F. Shchegolev, V. N. Laukhin, P. A. Kononovich, M. V. Kartsovnic, A. V. Zvarykina, and L. I. Buravov, *Pis'ma Zh. Eksp. Teor. Fiz.* **39**, 12 (1984).

4) H. Kobayashi, R. Kato, T. Mori, A. Kobayashi, Y. Sasaki, G. Saito, T. Enoki, and H. Inokuchi, *Mol. Cryst. Liq. Cryst.*, **107**, 33 (1983).

5) T. Mori, A. Kobayashi, Y. Sasaki, H. Kobayashi, G. Saito, and H. Inokuchi, *Bull. Chem. Soc. Jpn.*, **57**, 627 (1984).

6) T. Mori, A. Kobayashi, Y. Sasaki, H. Kobayashi. G. Saito, and H. Inokuchi, *Chem. Lett.*, **1984**, 957.

7) G. Saito, H. Kumagai, C. Katayama, C, Tanaka, J. Tanaka, P. Wu, T. Mori, T. Enoki, and H. Inokuchi, to be published.

8) C. Katayama, M. Honda, H. Kumagai, J. Tanaka, G. Saito, and H. Inokuchi, *Bull. Chem. Soc. Jpn.*, **58**, 2272 (1985).

9) P. Coppens, *"Extended Linear Chain Compounds I,"* ed by J. S. Miller, Plenum (1982), p. 333.

10) P. M. Chaikin and J. F. Kwak, *Rev. Sci. Instrum.*, **46**, 218 (1975).

11) K. Carneiro J. C. Scott, and E. M. Engler, *Solid State Commun.*, **50**, 477 (1984).

12) J. F. Kwak, *Phys. Rev.*, **B26**, 4789 (1982).

13) T. Mori, A. Kobayashi, Y. Sasaki, R. Kato, and H. Kobayashi, *Chem. Lett.*, **1984**, 1335.

14) R. Kato, H. Kobayashi, T. Mori, A. Kobayashi, and Y. Sasaki, *Solid State Commun.*, **55**, 387 (1985).